Holographic Turbulence

Allan Adams, Paul M. Chesler, and Hong Liu
Department of Physics, Massachusetts Institute of Technology, Cambridge, Massachusetts 02139, USA
(Received 9 September 2013; revised manuscript received 25 November 2013; published 14 April 2014)

We construct turbulent black holes in asymptotically AdS_4 spacetime by numerically solving Einstein's equations. Using the AdS/CFT correspondence we find that both the dual holographic fluid and bulk geometry display signatures of an inverse cascade with the bulk geometry being well approximated by the fluid-gravity gradient expansion. We argue that statistically steady-state black holes dual to d dimensional turbulent flows have horizons whose area growth has a fractal-like structure with fractal dimension $D = d + 4/3$.

DOI: 10.1103/PhysRevLett.112.151602 PACS numbers: 11.25.Tq, 04.50.Gh

Introduction.—According to holography, turbulent flows in relativistic boundary conformal field theories should be dual to dynamical black hole solutions in asymptotically AdS_{d+2} spacetime with d the number of spatial dimensions the turbulent flow lives in. This immediately raises many interesting questions about gravitational dynamics. For example, what distinguishes turbulent black holes from nonturbulent ones? What is the gravitational origin of energy cascades and the Kolmogorov scaling observed in turbulent fluid flows?

Gravitational dynamics can also provide insight into turbulence itself. For superfluids, where vortices are not governed by hydrodynamics, holography has demonstrated there can be a direct cascade to the UV even in two dimensional turbulence [1]. Likewise, having control of regimes beyond the hydrodynamic description of turbulence of normal fluids may allow one to study the domain of validity and the late-time regularity of solutions to the Navier-Stokes equation.

In this Letter we take a first step towards studying holographic turbulence by numerically constructing black hole solutions in asymptotically AdS_4 spacetime dual to $d = 2$ turbulent flows, where energy flows from the UV to the IR in an inverse cascade. We propose a simple geometric measure to distinguish turbulent black holes from nonturbulent ones: the horizon of a turbulent black hole exhibits a fractal-like structure with effective fractal dimension $D = d + 4/3$. The $4/3$ in this formula can be understood as the geometric counterpart of the rapid entropy growth implied by the Kolmogorov scaling.

Numerics and gravitational description.—We generate turbulent evolution by solving Einstein's equations

$$R_{MN} - \frac{1}{2}G_{MN}(R - 2\Lambda) = 0, \tag{1}$$

with cosmological constant $\Lambda = -3$. Here and below upper case latin indices run over all AdS spacetime coordinates, Greek indices run over boundary spacetime coordinates, and lower case latin indices run over spatial coordinates. Our numerical scheme for solving Einstein's equations is outlined in [2–4] and will be further elaborated on in a coming paper [5]. In what follows we focus on some of the salient details.

We employ a characteristic formulation of Einstein's equations and choose the metric ansatz

$$ds^2 = r^2 g_{\mu\nu}(x,r)dx^\mu dx^\nu + 2drdt, \tag{2}$$

with $t \equiv x^0$. The coordinate r is the AdS radial coordinate with $r = \infty$ corresponding the AdS boundary. The ansatz (2) is invariant under the residual diffeomorphism $r \to r + \xi(x)$ for arbitrary $\xi(x)$. Since the geometry we study contains a black brane, we fix the residual diffeomorphism invariance by demanding the apparent horizon be at $r = 1$. Horizon excision is then performed by restricting the computational domain to $r \geq 1$.

The AdS boundary is causal and therefore boundary conditions must be imposed there. Solving Einstein's equations with a series expansion about $r = \infty$, one finds an asymptotic expansion of the form $g_{\mu\nu}(x,r) = g^{(0)}_{\mu\nu}(x) + \cdots + g^{(3)}_{\mu\nu}(x)/r^3 + \cdots$. All omitted terms in the expansion are determined by $g^{(0)}_{\mu\nu}(x)$ and $g^{(3)}_{\mu\nu}(x)$. The coefficient $g^{(0)}_{\mu\nu}(x)$ corresponds to the metric the dual turbulent flow lives in. Hence, we choose the boundary condition $\lim_{r\to\infty} g_{\mu\nu}(x,r) = \eta_{\mu\nu}$. The coefficient $g^{(3)}_{\mu\nu}(x)$ is determined by solving Einstein's equations and encodes the expectation value of the boundary stress tensor [6]

$$\langle T_{\mu\nu}(x)\rangle = \frac{3}{16\pi G_N}\left[g^{(3)}_{\mu\nu}(x) + \frac{1}{3}\eta_{\mu\nu}g^{(3)}_{00}(x)\right], \tag{3}$$

where G_N is Newton's constant.

We choose initial data corresponding to a locally boosted black brane with metric

$$g_{\mu\nu} = (\mathcal{R}/r)^2[\eta_{\mu\nu} + (r_h/\mathcal{R})^3 u_\mu u_\nu], \tag{4}$$

where $u_\mu(x)$ is the local boost velocity and $r_h(x) = 4\pi T(x)/3$, with $T(x)$ the local temperature of the brane. The function $\mathcal{R}$ satisfies $\partial\mathcal{R}/\partial r = [1 + (r_h/\mathcal{R})^3 \boldsymbol{u}^2]^{1/2}$.

We work in a periodic spatial box of size Δx. We choose the initial boost velocity

$$u_x(x, y) = \delta u_x(x, y), \qquad u_y(x, y) = \cos Qx + \delta u_y(x, y), \tag{5}$$

with $Q = 20\pi/\Delta x$. The small fluctuations δu_i are present to break the symmetry of the initial conditions. We choose δu_i to be a sum of the first four spatial Fourier modes with random coefficients and phases and adjust the overall amplitude of δu_i such that $|\delta u_i| < 1/5$. These initial conditions are unstable and capable of producing subsequent turbulent evolution if the Reynolds number Re is sufficiently large. For our initial conditions Re $\sim T\Delta x$. We choose box size $\Delta x = 1500$ and the initial temperature $4\pi T/3 = 1$. We discretize Einstein's equations using pseudospectral methods and represent the radial dependence in terms of an expansion of 20 Chebyshev polynomials and the $x - y$ dependence in terms of an expansion of 305 plane waves. We then evolve the discretized geometry for 3001 units of time.

Results and discussion.—In Fig. 1 we plot of the boundary vorticity $\omega \equiv \epsilon^{\mu\nu\alpha} u_\mu \partial_\nu u_\alpha$ at three different times. To compute the vorticity we first extract the boundary stress tensor $\langle T^{\mu\nu} \rangle$ from the metric via Eq. (3). We then define the fluid velocity u^μ as the normalized ($u^2 = -1$) future-directed timelike eigenvector of $\langle T^\mu_\nu \rangle$,

$$\langle T^\mu_\nu \rangle u^\nu = -\varepsilon u^\mu, \tag{6}$$

with ε the proper energy density.

During times $t = 0$ through $t \sim 700$ our system experiences an instability which destroys the initial sinusoidal structure in the initial data (5) and drives the system into turbulent evolution. As seen in Fig. 1, by time $t = 2000$ there are many vortices present with fluid rotating clockwise (red) and counterclockwise (blue). During the latter evolution seen at times $t = 2496$ and 3001 isolated vortices with the same rotation tend to merge together to produce larger and larger vortices. The merging of vortices of like rotation to produce larger vortices is a tell tale signature of an inverse cascade.

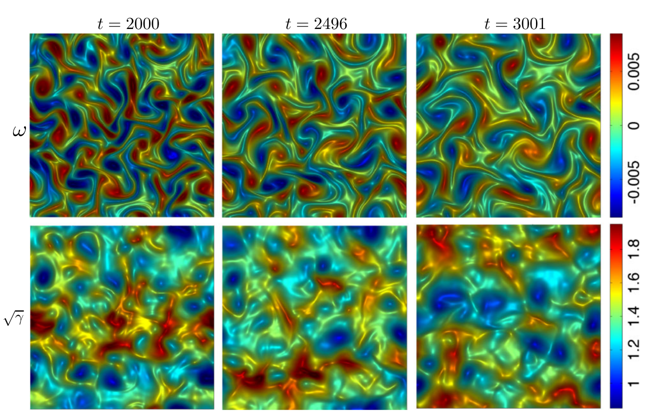

FIG. 1 (color online). Left: The boundary vorticity ω at 3 times. Right: the horizon area element $\sqrt{\gamma}$ at the same 3 times.

It is interesting to compare our results to the Kolmogorov theory of turbulence. A classic result from Kolmogorov's theory is that for driven steady-state turbulence the power spectrum $\mathcal{P}$ of the fluid velocity,

$$\mathcal{P}(t, k) \equiv \frac{\partial}{\partial k} \int_{|\boldsymbol{k}'| \le k} \frac{d^d k'}{(2\pi)^d} |\tilde{\boldsymbol{u}}(t, \boldsymbol{k}')|^2, \tag{7}$$

with $\tilde{\boldsymbol{u}}(t, \boldsymbol{k}) \equiv \int d^d x \boldsymbol{u}(t, \boldsymbol{x}) e^{-i\boldsymbol{k}\cdot\boldsymbol{x}}$, obeys the scaling

$$\mathcal{P}(t, k) \sim k^{-5/3}, \tag{8}$$

in an inertial range $k \in (\Lambda_-, \Lambda_+)$. Despite the fact that our system is not driven or in a steady-state configuration we do see hints of the Kolmogorov scaling. In Fig. 2 we plot $\mathcal{P}$ at time $t = 1008$. Our numerical results are consistent with the scaling (8) in the inertial range $k \in (0.025, 0.055)$. As we are not driving the system, evidence of the $k^{-5/3}$ scaling is transient and destroyed first in the UV, with the UV knee at $k = 0.055$ shifting to the IR as time progresses. Beyond the inertial range the spectrum decreases like $\mathcal{P} \sim k^{-p}$ with $p \sim 5$ until $k \sim 0.15$.

The inverse cascade also manifests itself in gravitational quantities. One interesting quantity to consider is the event horizon area element $\sqrt{\gamma} \equiv \sqrt{\gamma_{ij}}$, where γ_{ij} in the induced horizon metric. In our coordinate system and in the limit of large Reynolds number Re—a requirement for turbulent evolution—the event and apparent horizons approximately coincide at $r = 1$ and $\gamma_{ij} \approx g_{ij}|_{r=1}$ [7]. Also included in Fig. 1 are plots of $\sqrt{\gamma}$. At $t = 2000$ $\sqrt{\gamma}$ exhibits structure over a large hierarchy of scales and is fractal-like in appearance. We comment more on this further below. However, as time progresses $\sqrt{\gamma}$ becomes smoother and smoother just as the fluid vorticity ω does due to the inverse cascade.

The velocity power spectrum $\mathcal{P}$ also imprints itself in bulk quantities. One quantity to consider is the extrinsic curvature Θ_{MN} of the event horizon. Θ_{MN} can be

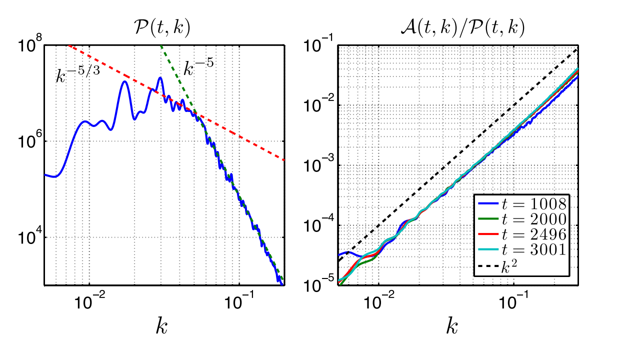

FIG. 2 (color online). Left: The velocity power spectrum $\mathcal{P}$ at time $t = 1008$. Right: The normalized horizon curvature power spectrum A/P at 4 different times.

constructed from the null normal n_M to the horizon and an auxiliary null vector ℓ_M whose normalization is conveniently chosen to satisfy $\ell_M n^M = -1$. The extrinsic curvature is then given by $\Theta_{MN} \equiv \Pi^P_M \Pi^Q_N \nabla_P n_Q$ with $\Pi^M_N \equiv \delta^M_N + \ell^M n_N$. Since the horizon is at $r \approx 1$ we choose $n_M dx^M = dr$ and $\ell_M dx^M = -dt$. The horizon curvature satisfies $\Theta^M_N \Theta^N_M = \Theta^i_j \Theta^j_i$. For later convenience, we define the rescaled traceless horizon curvature $\theta^i_j \equiv \sqrt{(\gamma/\kappa^2)}\Sigma^i_j$, where $\Sigma^i_j \equiv \Theta^i_j - (1/d)\Theta^n_n \delta^i_j$ is the traceless part of the extrinsic curvature and κ is defined by the geodesic equation $n^M \nabla_M n_Q = \kappa n_Q$.

Also included in Fig. 2 are plots of $\mathcal{A}(t,k)/P(t,k)$ where the horizon curvature power spectrum is

$$\mathcal{A}(t,k) \equiv \frac{\partial}{\partial k} \int_{|\boldsymbol{k}'| \le k} \frac{d^d k'}{(2\pi)^d} \tilde{\theta}^{*i}_j(t,\boldsymbol{k}') \tilde{\theta}^j_i(t,\boldsymbol{k}'), \tag{9}$$

with $\tilde{\theta}^i_j \equiv \int d^d x \theta^i_j e^{-i\boldsymbol{k}\cdot\boldsymbol{x}}$. As Fig. 2 makes clear, our numerical results are consistent with

$$\mathcal{A}(t,k) \sim k^2 P(t,k). \tag{10}$$

Evidently, bulk quantities are correlated with boundary quantities. As we detail below, this is a consequence of the applicability of the fluid-gravity correspondence.

Both qualitative and quantitative aspects of our results can be understood in terms of relativistic conformal hydrodynamics and the fluid-gravity correspondence. In the limit of asymptotically slowly varying fields (compared to the dissipative scale set by the local temperature T of the system) Einstein's equations (1) can be solved perturbatively with a gradient expansion $g_{\mu\nu}(x^\mu, r) = \sum_n g^{(n)}_{\mu\nu}(x^\mu, r)$, where $g^{(n)}_{\mu\nu}$ is order $(\partial/\partial x^\mu)^n$ in boundary spacetime derivatives [8]. The expansion coefficients $g^{(n)}_{\mu\nu}$ can be expressed in terms of the boundary quantities T and u^μ and their spacetime derivatives. The leading order term $g^{(0)}_{\mu\nu}$ is just the locally boosted black brane (4). Likewise, via Eq. (3) the bulk gradient expansion encodes the boundary stress gradient expansion $\langle T_{\mu\nu}(x^\mu)\rangle = \sum_n T^{(n)}_{\mu\nu}(x^\mu)$. The expansion coefficient $T^{(0)}_{\mu\nu} = (\varepsilon/d)[\eta_{\mu\nu} + (d+1)u_\mu u_\nu]$ is the stress tensor of ideal conformal hydrodynamics. Likewise, $T^{(1)}_{\mu\nu} = -\eta\sigma_{\mu\nu}$ is the viscous stress tensor of conformal hydrodynamics with η the shear viscosity and $\sigma_{\mu\nu}$ the shear tensor given below in (15). The underlying evolution of u^μ and T and hence the bulk geometry is governed by conservation of the boundary stress tensor. Hence, at leading order in gradients the evolution of u^μ and T is governed by ideal relativistic hydrodynamics and the geometry is given by the boosted black brane metric (4). Indeed, it was recently demonstrated in [9] that turbulence in $d = 2$ ideal conformal relativistic hydrodynamics gives rise to an inverse cascade and exhibits the Kolmogorov scaling (8) with the former a consequence of enstrophy conservation.

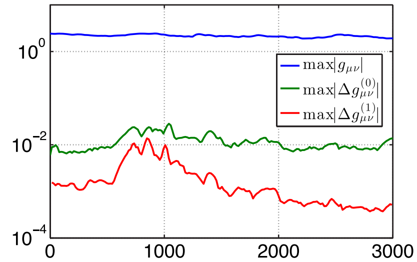

FIG. 3 (color online). Time evolution of the maximum difference between the exact metric and 0th and 1st order gradient expansion.

We find that our numerical metric $g_{\mu\nu}$ is very well approximated by the fluid-gravity gradient expansion. To perform the comparison, via Eq. (6) we extract u^μ and ε [and hence $T = (8\pi G_{\mathrm{N}}\varepsilon)^{1/3}$] from $\langle T^{\mu\nu}\rangle$. We then use u^μ and T to construct the expansion functions $g^{(n)}_{\mu\nu}$ computed in [10]. We then take the difference $\Delta g^{(N)}_{\mu\nu} \equiv g_{\mu\nu} - \sum_{m=0}^N g^{(m)}_{\mu\nu}$ and define the Nth order error to be $\max\{|\Delta g^{(N)}_{\mu\nu}|\}$ at each time t. As shown in Fig. 3, the boosted black brane metric (4) approximates the geometry at the 1% level. Including first order gradient corrections further decreases the size of the error.

It is natural that $d = 2$ turbulent evolution gives rise to dual geometries well approximated by locally boosted black branes. First of all, irrespective of d, turbulent flows require Reynolds number $\mathrm{Re} \gg 1$, or, equivalently, very small gradients compared to T. This is precisely the regime where the gradient expansions of fluid-gravity should be well behaved. Second, the inverse cascade of $d = 2$ turbulence implies that gradients become smaller and smaller as energy cascades from the UV to the IR. Therefore, once the inverse cascade has developed, the fluid-gravity expansion should become better and better behaved as time progresses. This is precisely what we observe in Fig. 3. Therefore, Fig. 3 provides a quantitative measure of how the bulk geometry (and, hence, $\sqrt{\gamma}$) become smoother as time progresses.

At least for $d = 2$ the above observation has powerful consequences for studying turbulent black holes. Instead of numerically solving the equations of general relativity one can simply study the equations of hydrodynamics and construct the bulk geometry via the fluid-gravity gradient expansion. This is particularly illuminating in the limit of nonrelativistic fluid velocities $|\boldsymbol{u}| \ll 1$, where the bulk geometry and boundary stress are asymptotically close to equilibrium. As shown in [11], under the rescalings $t \to t/s^2$, $\boldsymbol{x} \to \boldsymbol{x}/s$, $\boldsymbol{u} \to s\boldsymbol{u}$, $\delta T \to s^2 \delta T$, with δT the variation in the temperature away from equilibrium, in the limit $s \to 0$, the boundary evolution of δT and u^μ implied by the fluid-gravity correspondence reduces to the nonrelativistic incompressible Navier-Stokes equation. Indeed, the above rescalings are symmetries of the Navier-Stokes equation. Likewise, in the $s \to 0$ limit the geometry dual to the Navier-Stokes equation is encoded in the expansion functions $g^{(0)}_{\mu\nu}$

and $g^{(1)}_{\mu\nu}$, which are known analytically [8,10]. At least for $d = 2$, where is it well known that solutions to the Navier-Stokes equation are regular, we therefore expect many known results from classic studies of turbulence—such as the Kolmogorov scaling (8)—to carry over naturally and semianalytically to gravity.

As an illustration of the above point we now turn our attention to the horizon of turbulent black holes and argue that the Kolmogorov scaling (8) together with the relation (10) implies that the turbulent horizons are fractal-like in nature with noninterger fractal dimension. To augment our numerical evidence of (8) and (10) we assume the validity of the fluid-gravity gradient expansion for any d and that the system is driven by an external force into a statistically steady-state configuration and that the Kolmogorov scaling applies over an arbitrarily large and static inertial range. Within the gravitational description the driving can be accomplished by a time-dependent deformation of the boundary geometry [3,11].

The fractal dimension of the horizon can be extracted from the horizon area. Introducing a spatial regulator δx, one could compute the horizon area A via the Riemann sum $A \approx \Sigma_i \sqrt{\gamma(x_i)}\Delta^d x_i$, where each element $\Delta^d x_i \sim (\delta x)^d$. The fractal dimension D is defined by the scaling

$$A \sim (\delta x)^{d-D}, \tag{11}$$

in the $\delta x \to 0$ limit.

To see how the Kolmogorov scaling (8) implies the horizon has a fractal structure we employ the Raychaudhuri equation,

$$\kappa \mathcal{L}_n \sqrt{\gamma} + \frac{\zeta}{\sqrt{\gamma}}(\mathcal{L}_n \sqrt{\gamma})^2 - \mathcal{L}_n^2 \sqrt{\gamma} = \sqrt{\gamma}\Sigma^i_j \Sigma^j_i, \tag{12}$$

which relates the change in the horizon's area element $\sqrt{\gamma}$ to the traceless part of the horizon's extrinsic curvature Σ^i_j. Here, $\mathcal{L}_n \equiv n^M \partial_M$ is the Lie derivative with respect to the null normal to the horizon n_M and $\zeta = (d-1)/d$. In the hydrodynamic limit of slowly varying fields salient to turbulent flows, the Raychaudhuri equation simplifies to $\mathcal{L}_n \sqrt{\gamma} = (\sqrt{\gamma}/\kappa)\Sigma^i_j \Sigma^j_i$. Integrating over the horizon, it follows that the rate of change of the horizon area A is

$$\frac{dA}{dt} = \int d^d x \frac{\sqrt{\gamma}}{\kappa} \Sigma^i_j \Sigma^j_i = \int_0^\infty dk \mathcal{A}(t,k), \tag{13}$$

where $\mathcal{A}$ is given in (9). We therefore see that $\mathcal{A}$ encodes the growth of the horizon area.

Using the locally boosted black brane metric (4), Σ^i_j can be computed as a gradient expansion. For geometries dual to fluid flows in d spatial dimensions the leading order results read [12]

$$\sqrt{\frac{\gamma}{\kappa^2}}\Sigma^i_j = \frac{1}{\sqrt{2\pi T}}\left(\frac{4\pi T}{d+1}\right)^{d/2}\left[\sigma^i_j + \frac{u^i}{u^0}\sigma^0_j\right] + O(\partial^2), \tag{14}$$

with $\sigma^\mu_\nu \equiv \eta^{\mu\alpha}\sigma_{\alpha\nu}$ and $\sigma_{\mu\nu}$ the hydrodynamic shear

$$\sigma_{\mu\nu} = \partial_{(\mu}u_{\nu)} + u_{(\mu}u^\rho \partial_\rho u_{\nu)} - \frac{1}{d}\partial_\alpha u^\alpha [\eta_{\mu\nu} + u_\mu u_\nu], \tag{15}$$

which satisfies $u^\mu \sigma_{\mu\nu} = 0$ and $\eta^{\mu\nu}\sigma_{\mu\nu} = 0$. Using (9) and (14) we see that at leading order in gradients $\mathcal{A}(t,k)$ is the power spectrum of $(2\pi T)^{-1/2}[4\pi T/(d+1)]^{d/2}\sigma^\mu_\nu$. Counting derivatives we see that (10) must be satisfied at leading order in gradients, just as demonstrated in Fig. 2.

Assuming that the system is driven into a steady state and the Kolmogorov scaling (8) applies, from (10) we see that for any d we have $\mathcal{A} \sim k^{1/3}$. Inserting a UV regulator into the momentum integral in (13) at $k = k_{\max}$ we conclude that for $k_{\max} \in (\Lambda_-, \Lambda_+)$

$$dA(k_{\max})/dt \sim k_{\max}^{4/3}. \tag{16}$$

Identifying $\delta x \sim 1/k_{\max}$ we conclude from (11) that the area grows in time as if the horizon has fractal dimension

$$D = d + 4/3. \tag{17}$$

Let us reiterate the features of our systems which make the horizon fractal: (i) UV-sensitive area, (ii) scaling in coordinate and momentum space (16), and (iii) statistical translational invariance. The result (17) is a bit peculiar as it is larger than the number of spatial dimensions of the whole spacetime. But note that we are considering a null hypersurface and thus the standard statement that the fractal dimension should be smaller than the dimension of the embedding space does not immediately apply [13]. It would be interesting to understand this better.

The origin of the fractal-like structure of the horizon is easy to understand. It is well known from fluid mechanics that turbulent flows have a fractal-like structure with large vortices being composed of smaller vortices which are themselves composed of smaller vortices and so on. This behavior can be seen in the plots of the vorticity in Fig. 1. Via the fluid-gravity gradient expansions this fractal-like structure imprints itself on the bulk geometry. Moreover, upon using Hawking's formula to relate the horizon area to entropy, the Raychaudhuri equation (13) combined with (14) translates into the familiar expression for entropy growth in hydrodynamics $dS/dt = \int d^d x (2\eta/T)\sigma_{\mu\nu}\sigma^{\mu\nu}$ with η the shear viscosity of the fluid. Thus the fractal horizon can be understood as the geometric counterpart of the familiar fact that turbulent flows generate entropy much more rapidly than laminar flows with the same rate of energy dissipation. Moreover, the size of the domain $k_{\max} \in (\Lambda_-, \Lambda_+)$ in which the scaling (16) applies encodes the hierarchy of scales in which the horizon contains self-similar structures. The UV terminus Λ_+ of the inertial range is bounded by the dissipative scale T, where hydrodynamics breaks down [14]. However, the IR terminus of the scaling (16) is bounded only by the system size. Therefore, the scaling (16) can be made to apply over an unboundedly large domain and the horizon can have geometric features over an unboundedly large hierarchy of scales.

We acknowledge helpful conversations with Christopher Herzog, Veronika Hubeny, Luis Lehner, Mukund Rangamani, and Laurence Yaffe. A. A. thanks the Aspen Center for Physics for hospitality. The work of A. A. is supported in part by the U.S. Department of Energy (DOE) under cooperative research Agreement No. DE-FC02-94ER40818. The work of P. M. C. is supported by a Pappalardo Fellowship in Physics at MIT. The work of H. L. is partially supported by a Simons Fellowship and by the U.S. Department of Energy (DOE) under cooperative research Agreement No. DE-FG0205ER41360.

[1] A. Adams, P. M. Chesler, and H. Liu, Science **341**, 368 (2012).
[2] P. M. Chesler and L. G. Yaffe, Phys. Rev. Lett. **106**, 021601 (2011).
[3] P. M. Chesler and L. G. Yaffe, Phys. Rev. Lett. **102**, 211601 (2009).
[4] V. Cardoso*et al.*, Classical Quantum Gravity **29**, 244001 (2012).
[5] P. M. Chesler and L. G. Yaffe, arXiv:1309.1439.
[6] S. de Haro, S. N. Solodukhin, and K. Skenderis, Commun. Math. Phys. **217**, 595 (2001).
[7] In the fluid-gravity gradient expansion the apparent and event horizons coincide at first order in gradients. Hence, their positions should coincide when gradients become asymptotically small, which occurs when Re $\to \infty$.
[8] S. Bhattacharyya, V. E. Hubeny, S. Minwalla, and M. Rangamani, J. High Energy Phys. 02 (2008) 045.
[9] F. Carrasco, L. Lehner, R. C. Myers, O. Reula, and A. Singh, Phys. Rev. D **86**, 126006 (2012).
[10] M. Van Raamsdonk, J. High Energy Phys. 05 (2008) 106.
[11] S. Bhattacharyya, S. Minwalla, and S. R. Wadia, J. High Energy Phys. 08 (2009) 059.
[12] C. Eling and Y. Oz, J. High Energy Phys. 02 (2010) 069.
[13] Standard definitions of fractal dimension require embedding the fractal in a higher dimension space. Such definitions cannot be applied to our fractal, a Lorentzian null hypersurface, whose geometry is known intrinsically. However, we believe our definition is equivalent to the standard box counting definition for a fractal satisfying the three features mentioned below (17).
[14] We note, however, that the constant of integration one gets from integrating (16) is of order T^d, which is the area element of an equilibrium black brane. Hence, the $k_{\max}^{4/3}$ scaling of the horizon area never dominates over the T^d constant and the scaling (11) is never exactly satisfied in the large $k_{\max}$ limit.